metals

MDPI

Article

Mineralogical Characterisation of Copper Slag and Phase Transformation after Carbocatalytic Reduction for Hydrometallurgical Extraction of Copper and Cobalt

Tina Chanda Phiri, Pritam Singh and Aleksandar N. Nikoloski *

Centre for Water Energy and Waste, Harry Butler Institute, School of Engineering and Energy, Murdoch University, 90 South Street, Murdoch, WA 6150, Australia; t.phiri@murdoch.edu.au (T.C.P.); p.singh@murdoch.edu.au (P.S.)

* Correspondence: a.nikoloski@murdoch.edu.au

Abstract: Copper smelting slag is a significant potential resource for cobalt and copper. The recovery of copper and cobalt from copper slag could significantly augment the supply of these metals, which are essential to facilitating the transition to green energy while simultaneously addressing environmental concerns regarding slag disposal. However, the complex mineral composition of copper slag poses an enormous challenge. This study investigated the mineralogical and chemical characteristics of copper slag, which are vital for devising the most effective processing techniques. XRD and FESEM-EDS were employed to examine the morphologies of copper slag before and after the reduction process. The effects of borax and charcoal (carbocatalytic) reduction on phase transformation were evaluated. The XRD analysis revealed that the primary phases in the copper slag were Fe_2SiO_4 and Fe_3O_4. The FESEM-EDS analysis verified the presence of these phases and yielded supplementary details regarding metal embedment in the Fe_2SiO_4, Fe_3O_4, and Cu phases. The carbocatalytic reduction process expedited the transformation of copper slag microstructures from crystalline dendritic to amorphous and metallic phases. Finally, leaching experiments demonstrated the potential benefits of carbocatalytic reduction by yielding high extractions of Cu, Co, and Fe.

Keywords: copper slag; carbocatalytic reduction; mineralogical characterisation; phase transformation

Citation: Phiri, T.C.; Singh, P.; Nikoloski, A.N. Mineralogical Characterisation of Copper Slag and Phase Transformation after Carbocatalytic Reduction for Hydrometallurgical Extraction of Copper and Cobalt. *Metals* **2024**, *14*, 1119. https://doi.org/10.3390/met14101119

Academic Editor: Petros E. Tsakiridis

Received: 28 August 2024
Revised: 25 September 2024
Accepted: 27 September 2024
Published: 1 October 2024

1. Introduction

Confronted with increasing industrialisation and civilisation, humanity is constantly seeking innovative technologies for a sustainable future. As a result, the extraction of mineral resources has progressively escalated to keep pace with the rapid development of society, and a few of these resources are nearing exhaustion. As high-grade deposits deplete, larger amounts of ore must be mined to provide an adequate supply of raw mAterials, resulting in increased generation of metallurgical waste. Copper smelting slag is a significant metallurgical waste, with a global annual production of 37.7 million tonnes [1]. The disposal of these substantial volumes of slag is concerning due to the potential release of hazardous substances into the environment. Copper slag waste contains hazardous metals, which mAy be a source of pollution affecting surface water, soil, and groundwater [2–4]. This could have an adverse impact on human health and the loss of biodiversity.

Conversely, smelting slag contains a substantial quantity of valuable metals, mAking it a highly appealing alternative mineral resource to meet the growing demand for critical metals in social and economic development [2,3]. Therefore, it is increasingly necessary to reduce waste disposal by extracting valuable metals from the slag waste, thereby contributing to a sustainable future. However, unlike the primary ore, the complex mineralogy of copper slag waste, which primarily consists of mAgnetite and fayalite, mAkes it extremely difficult to extract metals from it [5–7]. Fayalite ($2FeO{\cdot}SiO_2$) is a stoichiometric compound that melts at 1208 °C [8]. The significant presence of fayalite in copper slag poses huge

processing challenges due to its high melting point, necessitating energy-intensive processing [9–11]. As a result, a significant amount of slag waste is still stored, which leads to the buildup of slag waste outside of smelters and wastes vital resources while also polluting the environment. Morphology, mineralogical characteristics, and metal distribution are critical factors to understanding the resource utilisation potential of copper smelting slag.

The mineralogical composition of copper slag and the associated distribution of heavy metals were studied by Zhang et al. [6]. Sequential extraction demonstrated that fayalite was more difficult to extract than mAgnetite and hedenbergite due to its significantly stronger binding ability with heavy metals [6]. Guo et al. [12] discovered that during the pyrometallurgical smelting of copper concentrates, heavy metals like Cu, Pb, and As interact with Fe_2SiO_4 to form a compact encapsulation state. Several studies discovered that copper slag contains various valuable metals dispersed across different phases [2,13,14]. Our previous study has demonstrated that copper slag contains substantial quantities of valuable metals dispersed in other phases, including 2.59 wt.% Al, 1.83 wt.% Zn, 1.67 wt.% Ag, 1.19 wt.% Cu, and 0.48 wt.% Co [3]. The mineralogical composition of copper slag is complicated by the presence of these valuable metals in the mAjority of stable oxides and silicates. [6] observed that the tightly bound state of hazardous metals in various phases is indistinct, mAking the identification of the primary bound phases of hazardous metals more challenging. Nevertheless, only a limited number of studies have comprehensively analysed the microstructure and predominant occurrence of metal phases in copper slag. Additionally, to date, there has been no research conducted on the phase transformation of copper slag using charcoal in the presence of borax (carbocatalytic reduction). The objective of this study was to examine the morphology of copper slag and phase transformation produced by carbocatalytic reduction (CCR), which is fundamental for optimising the efficiency of disintegration and metal extraction. The research involved the use of microscopic and spectroscopic techniques, as well as laboratory chemistry experiments. The morphology of and phases present in the copper slag were determined using X-ray diffraction (XRD). The mineral phases of Co, Cu, Ti, Ca, Mg, Al, Fe, and Si were identified, and their distribution was analysed using a field emission scanning electron microscope equipped with a spectrometer with X-ray energy dispersion (FESEM-EDS). Additionally, the potential effect of carbocatalytic reduction for enhanced metal extraction was assessed through leaching experiments on the product of the copper slag reduction. The results of this study are essential for gaining a theoretical understanding of the complex mineralogy and phase transformation of copper slag, which could help to develop technology for extracting copper and cobalt and reprocessing the accumulated waste.

2. Materials and Methods

2.1. Sample Preparation

The copper slag waste utilised in this study was sourced from the Nkana slag dump in Kitwe, Zambia. To obtain a more accurate representation of the sample, a total of 60 kg of copper slag was collected from different locations within the slag dump. The largest diameter of the slag samples was 4.5 cm. Two crushing stages were used, comprising primary and secondary crushing using a jaw crusher and a cone crusher, respectively. To achieve consistency in the composition, the crushed product was sampled using a Jones riffle and then placed in plastic bags weighing 3 kg each. Each 3 kg sample was ground for 180 min at a speed of 70 rpm in a ball mill. Following that, the ground sample was sieved to achieve a particle size smaller than 0.075 mm. The slag was subsequently sampled using a Jones riffle, then divided into smaller portions through coning and quartering techniques, and finally stored in 0.3 kg plastic containers for experimental investigations. All reagents used in the reduction process, leaching, and chemical analysis were of analytical grade. Charcoal was utilised as a preferred flux, as it could serve as a sustainable and environmentally friendly reducing agent. Our previous research revealed that charcoal possesses a high carbon content, along with significant volatile mAtter and minimal ash content [7]. These properties render it well-suited for use as an effective reducing agent

for copper slag. Anhydrous borax ($Na_2B_4O_7$) facilitated the reduction of copper slag at low temperature. The leaching experiments were performed in H_2SO_4 solution at ambient temperature. Charcoal was purchased from Bunnings Warehouse (Perth, Australia), while $Na_2B_4O_7$ and H_2SO_4 were supplied by Rowe Scientific (Wangara, Australia).

2.2. Characterisation

2.2.1. Chemical Composition of the Copper Slag

The analysis of the elemental content of the copper slag was conducted using inductively coupled plasma optical emission spectroscopy (ICP-OES). A portion of the slag was mixed with sodium peroxide (Na_2O_2) in a platinum crucible, and the resulting mixture was heated in a furnace at a temperature of 500 °C for a duration of one hour. The resulting sinter was dissolved in a solution of 3 M hydrochloric acid. The solution was diluted, filtered, and analysed using the ICP-OES. Hydrochloric acid and Na_2O_2 were purchased from Rowe Scientific. The results of a typical chemical composition analysis of copper slag using ICP-OES are presented in Table 1.

Table 1. Elemental analysis of copper smelting slag using ICP-OES (wt.%).

Cu	Co	Fe	Al	Mg	Mn	Ca	Pb	Zn	Ni
1.04	0.79	25.63	11.05	3.50	0.66	7.15	0.03	0.06	0.05

2.2.2. XRD Analysis of Copper Slag

The mineralogical and structural characteristics of slag samples were analysed by X-ray diffractometry (XRD) using a Rigaku SmartLab equipped with a PhotonMax high-flux rotating anode X-ray source (Tokyo, Japan), and a HyPix-3000 high-energy-resolution 2D multidimensional semiconductor detector. The acceleration voltage and electrical current were 35 kV and 20 mA, respectively. The 2-theta diffraction angle was scanned from 10° to 90°. The step angle and scanning speed were 0.01° and 8° min^{-1}, respectively. The diffraction peaks depicted in Figure 1 suggest that copper slag predominantly comprises fayalite and mAgnetite.

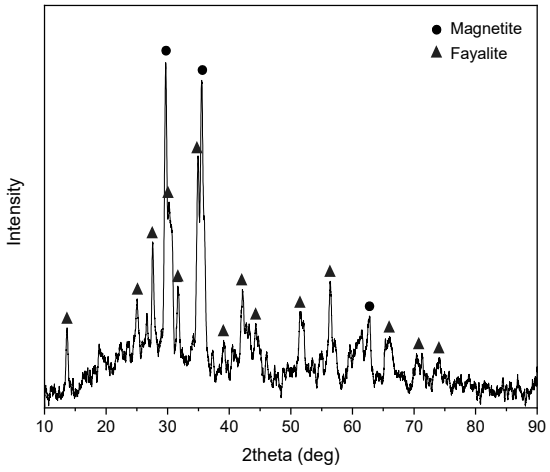

Figure 1. XRD pattern of copper slag.

2.2.3. FESEM-EDS Analyses of Copper Slag and Roasting Product

The morphology and elemental distribution of copper slag were examined using a field emission scanning electron microscope (FESEM, Tescan Mira3, Brno, Moravia, Czech Republic) combined with energy dispersive spectroscopy (EDS, Oxford Instruments X-Max 150 SDD X-ray detector with AZtec V5.1 software, Abingdon, Oxfordshire, UK) with a detection limit ranging from 0.1% to 1%. To achieve a clear and comprehensive examination of the distribution of phases and metals in copper slag, the samples were mounted using a

blend of epofix resin and epofix hardener. These mounts were then ground, polished to a smooth finish, and coated with platinum using a sputter coating technique to enhance conductivity before morphological analysis. The mounts were subsequently left for a period of 24 h to solidify. The Struers Tegramin 30 semi-automatic polisher (Struers, Copenhagen, Denmark) was used for the polishing process. The Piano 1200 pad (Buehler Illinois Tool Works, Lake Bluff, IL, USA) was utilised for the purpose of grinding to achieve a flat surface, which was subsequently polished using a diamond suspension. The polished sections of slag were examined using a backscattered electron (BSE) detector to capture images of specific areas of interest. Additionally, point analysis and mApping techniques were employed to gather EDS data, which was used to identify the elemental compositions and distributions of the different phases present in the slag. The BSE detector exhibits a variation in grey level that is contingent upon the phase's composition in relation to the average atomic number.

2.3. Treatment Methodology

2.3.1. Carbocatalytic Reduction of Copper Slag

Carbocatalytic reduction (CCR) is defined in this study as the reduction process that involves a mixture of charcoal and borax. The CCR process was achieved by thoroughly blending 50 g of finely ground copper slag with borax and charcoal. The borax dosage for different experiments was one of 0%, 10%, 20%, or 30% of copper slag mAss, while the charcoal dosage was one of 5%, 10%, 15%, or 20% of copper slag mAss. The heterogeneous samples were transferred into a graphite crucible, placed inside a muffle furnace, and subjected to thermal treatment. The temperatures employed were 800, 850, 900, 950, and 1000 °C, while the durations of reduction were 60, 90, 120, and 180 min. The product after roasting was cooled to ambient temperature prior to being pulverised into a fine powder.

2.3.2. Sulphuric Acid Leaching of the Feed Sample and Reduction Product

The feed sample was first leached in 2 M H_2SO_4 for a duration of 90 min at room temperature (25 °C), with a liquid–solid ratio of 4 mL/g. The carbocatalytic reduction product (under optimum conditions of 10% charcoal and 20% borax dosage at 850 °C for 90 min of reduction time) was also leached under the same optimum leaching conditions. A comprehensive analysis of the optimisation of borax dosage, charcoal addition, temperature, reduction time, acid concentration, and leaching time is provided in our previous study [7]. The leaching solution and residue were then separated through vacuum filtration, and the leach residue was rinsed with 200 mL of deionized water. The leach residue was collected on filter paper and subjected to desiccation in an oven at 70 °C. The leach residue of the product after the carbocatalytic reduction process was digested and analysed in accordance with the procedure described in Section 2.2.1. To prevent the metal ions from precipitating due to hydrolysis, the filtered leachates were mixed with a 2% hydrochloric acid (HCl) solution before being analysed for Co, Cu, and Fe concentrations using the ICP-OES. Following leach solution analysis, the results of the feed sample and product after carbocatalytic reduction were compared. The leachability of each valuable metal was assessed using a mAss balance and applying data obtained from the analysis of the copper slag feed, leach solution, and leach residue.

3. Results and Discussions

3.1. Morphological Characteristics and Phase Composition of Copper Slag

The morphological characteristics and phase composition of the copper slag feed sample were investigated using the FESEM-EDS. Figure 2 clearly shows three distinct phases: copper mAtte (point 1), mAgnetite (point 2), and silicate (point 3). Table 2 indicates the phase composition of the mAterial at points 1, 2, and 3 in Figure 2.

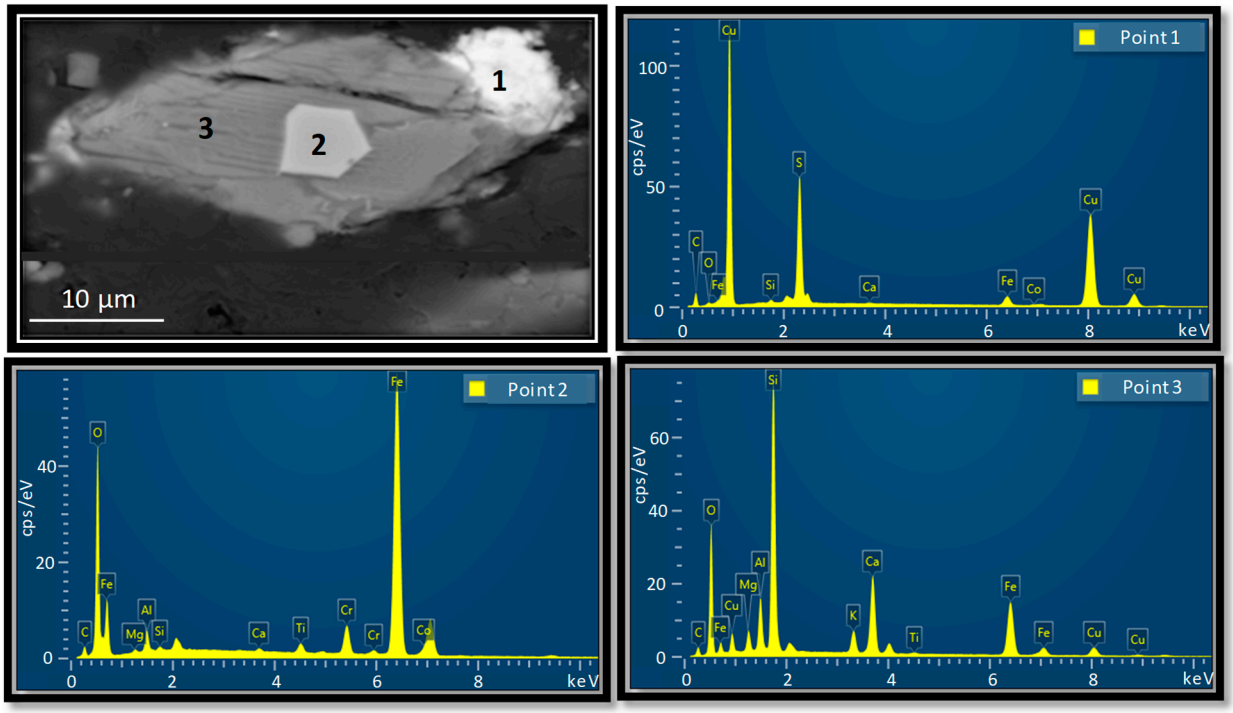

Figure 2. FESEM microstructure of the copper slag sample and EDS spectra of copper mAtte (Point 1), mAgnetite (Point 2), and silicate (Point 3).

Table 2. Elemental composition of the mAin phases in the copper slag in wt.% (Figure 2).

Mineral Phase	Point	Co	Cu	S	Fe	Si	O	Ca	Al	Mg	Ti	K
Copper mAtte	1	0.21	65.57	18.58	2.98	0.47	0.72	0.14				
Magnetite	2	1.36			58.26	0.24	21.75	0.24	1.81	0.35	0.97	
Silicate	3		4.42		15.55	22.36	37.64	9.5	4.56	2.16	0.22	2.53

The copper mAtte (Point 1) consisted primarily of copper and sulphur. The mAgnetite particle at point 2 exhibited a mAtrix consisting of iron oxide with metallic inclusions, including Co, Mg, Al, and Ti, as shown by the EDS analysis. The mAgnetite particle was encapsulated within the silicate mAtrix, indicating the simultaneous presence of multiple phases in the copper slag. Point 3 was identified as a silicate phase. The FESEM-EDS analysis revealed the existence of metallic elements, including Co, Cu, Mg, K, Al, Ti, and Fe, which are bound to both the mAgnetite and silicate structure. These findings indicate that the mineralogical composition of copper slag is extremely heterogenous and complex. This aligns with previous studies indicating that the mineral composition of copper slag is both chemically diverse and complicated [3–7,10,11,15].

3.2. Embedment of Metals in Mineral Phases in the Copper Slag

To illustrate the embedment of valuable metals in mineral phases, the phases of the polished surface of the copper slag were identified and analysed using backscattered electron (BSE) imaging. Figure 3a demonstrates the presence of various mineral phases interconnected within the copper slag. To obtain detailed BSE microstructure information, the mArked areas X, Y, and Z in Figure 3a were deconvoluted, and the results are presented as Figure 3b–d, respectively. The corresponding compositions at various points in Figure 3b,c are presented in Tables 3 and 4, respectively.

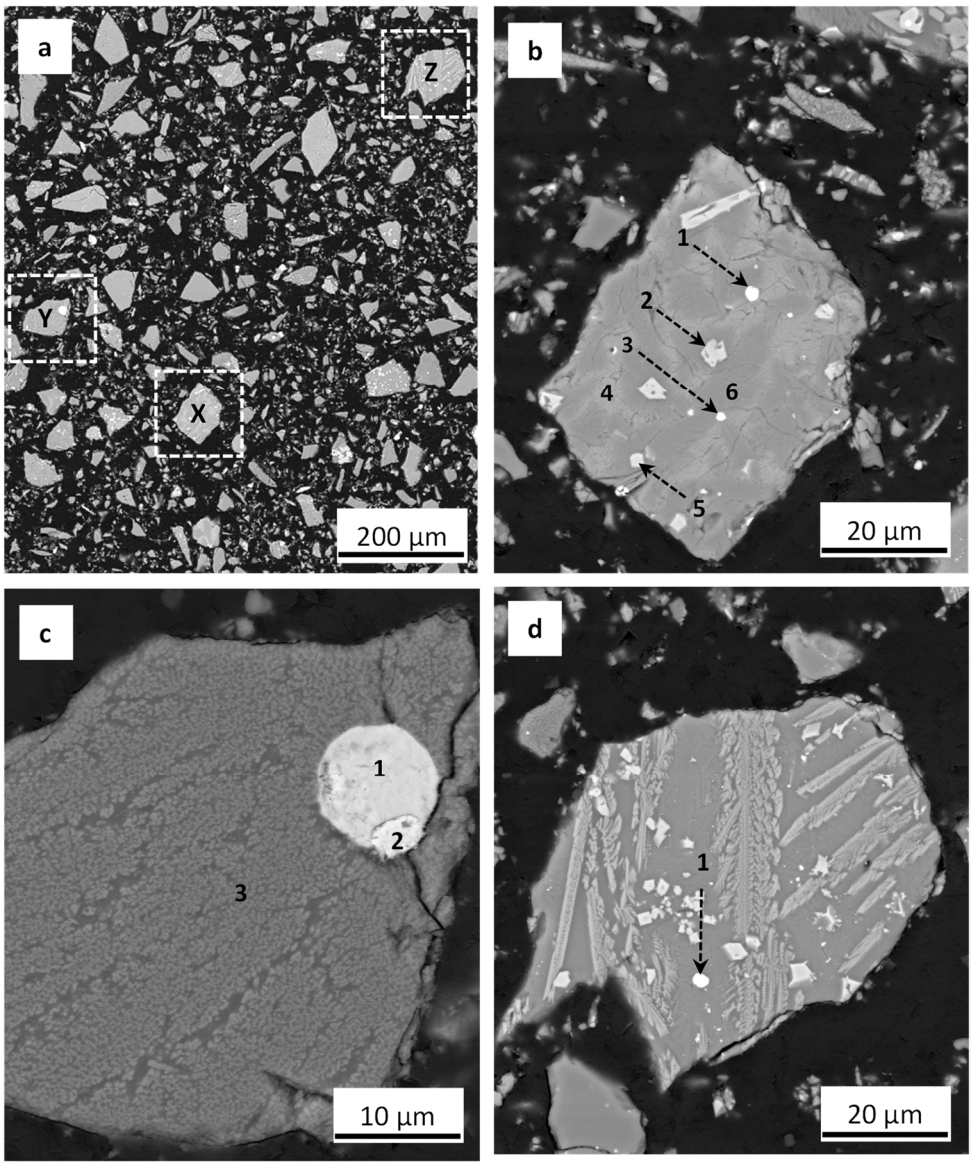

Figure 3. Backscattered electron micrograph of the polished surface in copper slag (**a**) and deconvoluted images of areas mArked X (**b**), Y (**c**), and Z (**d**).

Table 3. Elemental composition of the mAin phases in the copper slag in wt.% (Figure 3b).

Mineral Phase	Point	Co	Cu	S	Fe	Si	O	Ca	Al	Mg	Ti	K
Copper mAtte	1	0.38	57.56	20.8	11.01	2.34	4.76	0.6	0.64			0.46
Magnetite	2	1.85			51.33	3.94	24.87	1.43	2.49	0.34	1.14	1.08
Silicate	3	1.3	5.08	2.04	24.91	14.07	24.81	4.71	2.29	0.76	0.12	1.49
Silicate	4	1.25			31.11	16.29	28.37	2.51	3.9	0.39	0.14	3.52
Silicate	5	1.44			25.24	12.26	25.9	6	2.07	1.8	0.43	0.91
Silicate	6	1.32			20.9	19.44	31.46	7.98	3.43	2.41	0.16	1.18

Table 4. Elemental composition of the mAin phases in the copper slag in wt.% (Figure 3c).

Mineral Phase	Point	Co	Cu	S	Fe	Si	O	Ca	Al	Mg	Ti	K
Copper mAtte	1	0.11	73.52	18.36	2.5	0.08	0.67					
Copper metallic	2	0.14	89.62	0.12	3.17	0.37	1.38	0.08				
Silicate	3	1.05	0.54		22.4	23.25	40.9	1.73	5.17	2.25	0.45	2.82

3.2.1. Copper Phase Occurrence and Metal Embedment in Copper Slag

To evaluate the embedment of metals within the copper mineral phase of the copper slag, FESEM-EDS analysis was performed on the designated areas in Figure 3b,c. The back-scattered electron (BSE) micrographs in Figure 3b display micrometre-sized copper mineral particles embedded on the surfaces of a large, complex silicate glass fragment. Figure 3c shows a complex fragment interbedded within the silicate mAtrix. Tables 3 and 4 provide confirmation that copper mAtte and metallic copper were the primary mineral phases of copper in the copper slag and give their respective phase compositions at various points. The copper mineral phases were mAinly present as fine spherical white inclusions or prills (Figure 3b–d). The CuS is intergrown with enclosed CoS and various metals such as Fe, Ca, Al, K, and Si (Table 3). The copper phase exhibited particle sizes ranging from 5 to 20 μm. The small size of these particles presents a significant challenge in the separation of copper minerals from copper slag. In Table 4, it was observed that the copper phase contained a significant amount of copper, with distribution rates of 73.52 wt.% and 89.62 wt.% at points 1 and 2, respectively. Previous research has demonstrated that copper in the copper slag is present in the form of copper mAtte [2,13,14]. Copper mAtte was also found in association with iron (Table 3). Cobalt primarily existed in the copper phase as jaipurite (CoS) and as a metallic phase. The primary constituents of the copper phase were copper mAtte and metallic copper, along with small amounts of Co, Fe, Si, O, Ca, Al, and K (as shown in Tables 3 and 4).

3.2.2. Magnetite Phase Occurrence and Metal Embedment in Copper Slag

In Figure 3b, the area labelled as point 2 shows a tetrahedral mAgnetite phase containing metal inclusions, including Co, Mg, Al, Ti, Ca, K, and Si, which are encapsulated in the silicate assemblage. The EDS results of the various phase compositions of the points in Figure 3b are shown in Table 3. The mAgnetite particles exhibited dispersion and fineness and were embedded within the silicate phase. The mAgnetite phase, similar to the copper phase, appeared as microparticles measuring less than 20 μm in size. mAgnetite was identified as a perfect tetrahedron in the copper slag, as well as euhedral spinels (points 2 in Figures 2 and 3b). mAgnetite predominantly occurred interbedded with silicates, forming a cohesive structure with iron and other metallic elements. The concentration of iron was greater in the mAgnetite phase compared with the silicate phase. Measurements of electron paramagnetic resonance show that ferric iron (Fe^{3+}) exists in both the octahedral cation sites and the tetrahedral cation (silicon) sites, with slightly higher concentrations in the former [16]. Therefore, the high concentration of iron in the mAgnetite phase mAy be attributed to the presence of Fe^{3+} in the tetrahedral cation (silicon) sites. The observed tetrahedral geometries in Figure 3b align with this finding, indicating a high iron concentration of 51.33 wt.% (Point 2) in the mAgnetite phase compared with 24.91 wt.% (Point 3) in the silicate phase in Table 3. Cobalt exists primarily as cobalt ferrite ($CoFe_2O_4$) spinels in the mAgnetite phase. This suggests that cobalt is highly concentrated in the mineral structure of mAgnetite, with a cobalt content of 1.85 wt.% (Table 3).

3.2.3. Silicate Phase Occurrence and Metal Embedment in Copper Slag

The mineralogical composition of silicate phases in the copper slag exhibited diverse grey structures, primarily composed of fayalite (Fe_2SiO_4) and kirschsteinite ($CaFe_2SiO_4$), which are minerals belonging to the olivine group (Figure 3b and Tables 2–4). A closer examination of Figure 3b reveals that two phases are intermingling. The two phases can be differentiated based on their varying shades of grey. The brighter crystals correspond to the fayalite phase (Figure 3b, point 4), which is rich in iron and poor in calcium. The dark crystals correspond to the kirschsteinite phase (Figure 3b, point 6), which is rich in calcium and iron. This is confirmed by the EDS results shown in Table 3. Fayalite is an iron orthosilicate that possesses the crystal structure of olivine. Kirschsteinite is a crystalline silicate mineral that is grey in colour and has an orthorhombic crystal structure. Figure 3d displays a characteristic dendritic silicate structure on the glassy fragments,

with small sulphide, oxide, and metallic droplets embedded on the surface. The copper slag contained additional silicate phases that are classified as members of the pyroxene group, including clinopyroxene ((Ca, Mg, Fe, Na) (Mg, Fe, Al) (Si, Al)$_2$O$_6$), hedenbergite ($CaFeSi_2O_6$), diopside ($CaMgSi_2O_6$), and ferrosilite ($Fe_2Si_2O_6$). A significant number of metals were found contained in the silicate phase, including Co, Cu, Fe, Si, Ca, Mg, Al, Ti, and K. This is consistent with a recent study that found metals embedded in similar phases, primarily composed of crystalline silicate phases, including forsterite (Mg_2SiO_4) and fayalite (Fe_2SiO_4), as well as enstatite ($Mg_2Si_2O_6$) and ferrosilite [17]. In another study, Zhang et al. [6] found heavy metals embedded in the Fe_2SiO_4, Fe_3O_4, and $CaFeSi_2O_6$ phases, with fayalite having a significantly greater binding ability with heavy metals than the other phases.

3.2.4. Distribution of Cu, Co, and Fe in the mAin Phases of Copper Slag

The FESEM-EDS analysis revealed that the copper smelting slag predominantly contained silicate, mAgnetite, and copper phases. In this study, the silicate phase is defined as primarily fayalite and kirschsteinite, while the copper phase is composed of copper mAtte and metallic copper. The Co content was uniformly distributed in the mAgnetite, silicate, and copper mAtte phases with up to 1.85 wt.%, 1.44 wt.%, and 0.38 wt.%, respectively (Table 3). This finding aligns with the research conducted by [18], which demonstrated that the distribution of Co primarily occurs in the fayalite phase, specifically in the form of silicate and ferrite. The iron contents in the mAgnetite, silicate, and copper mAtte phases were up to 58.26 wt.%, 31.11 wt.%, and 11.01 wt.%, respectively (Tables 2 and 3). The copper content distribution percentages in silicate, copper mAtte, and metallic copper phases were 5.08 wt.%, 73.52 wt.%, and 89.62 wt.%, respectively (Tables 3 and 4). In another study, Zhang et al. [6] discovered that despite the significantly higher weight percentage of copper metal in iron phases compared with fayalite and mAgnetite minerals, fayalite exhibited a more robust tendency to bind heavy metals. The study discovered that 89.7% As, 85.0% Pb, and 76.9% Cu were tightly bound to the fayalite phase [6]. Previous studies have indicated that Cu has the potential to be integrated into the fayalite structure by displacing the active sites of Fe [6,9,19]. Examining the binary phase diagram of Cu and Fe, Zhou et al. [20] noted that both Cu and Fe exhibit miscible dissolution, which can be attributed to their comparable chemical structures. In this study, Cu was typically present in high concentrations in the copper phase, low concentrations in the silicate phase, and no copper was observed in the mAgnetite phase in the mArked areas of the feed sample (Tables 2–4). Meanwhile, the distribution of Co and Fe in the copper smelting slag was consistently found across all phases (Tables 3 and 4). The surfaces of the silicate and mAgnetite phases in Figure 3b–d contained a significant amount of embedded metallic phases. Tables 3 and 4 demonstrate the existence of metals incorporated within various phases in the copper slag, specifically Co, Cu, Fe, Ca, K, Al, Ti, and S. Moreover, the EDS results reveal the coexistence of multiple metallic phases, thereby confirming their presence in different phases.

3.3. Evaluation of Processing Technology Parameters

3.3.1. Effect of Borax Addition on Morphological Transformation

The effect of borax addition on morphological transformation of the copper slag was investigated in this study. The borax addition was varied in the range of 0%, 10%, 20%, and 30% with 10% charcoal at 850 °C reduction temperature for 90 min. Figure 4a–d displays the morphological features of the copper slag after the carbocatalytic reduction.

Figure 4a depicts a sample without borax addition, which exhibits microstructure comparable to the feed sample (Figure 3a). The sample displays skeletal, dendritic, or irregular crystals in the absence of borax, indicating that it mAy have been formed under a rapid cooling process. Figure 4b shows more regular spherical microparticles compared with Figure 4a due to the presence of 10% borax. However, certain regions still contained dendritic crystals, indicating that the phase transformation had yet to be completed. By increasing the borax addition to 20% and 30% (as shown in Figure 4c,d), a sample with

well-defined geometries and uniformly distributed spherical particles is obtained. The metallic grains, which are small and spherical in shape, are observed distributed between the particle boundary and the surface of the mAin structure. The reason can be ascribed to the decomposition of borax occurring within the copper slag phase, which then accelerates the reduction process. Furthermore, the ability of borax to decompose and its low melting point mAke it well-suited for the decomposition of high-temperature fayalite in the copper slag. Based on the experimental results, it can be inferred that the addition of borax has the potential to enhance the transformation of the dendritic crystalline silicate structure into an amorphous structure and metallic phase.

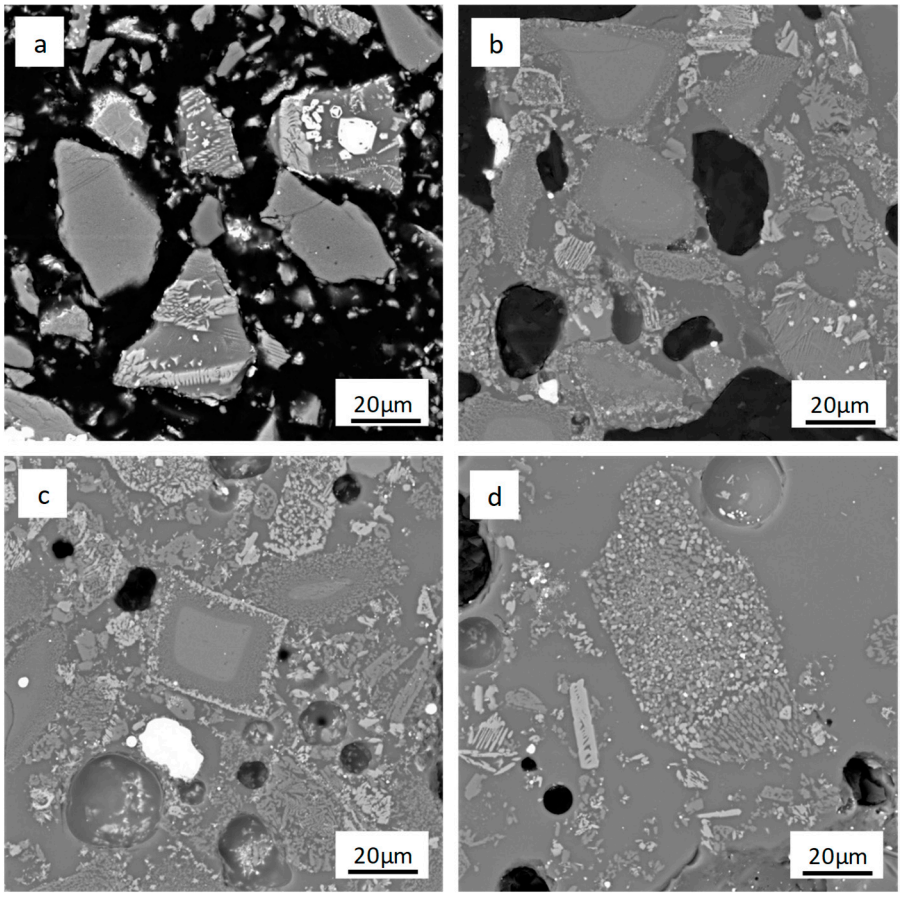

Figure 4. Effects of borax on morphological transformation with additions of 0% (**a**), 10% (**b**), 20% (**c**), and 30% (**d**) borax, with 10% charcoal and 850 °C reduction temperature.

3.3.2. Effect of Borax Addition on Phase Transformation

The phase transformation of copper slag during carbocatalytic reduction (CCR) with different amounts of borax was investigated, as shown in Figure 5. The copper slag was roasted at a temperature of 850 °C for a reduction time of 90 min, using 10% charcoal and 0%, 10%, 20%, and 30% borax ($Na_2B_4O_7$). In the absence of $Na_2B_4O_7$, the X-ray diffraction data indicated the coexistence of mAgnetite and fayalite phases (Figure 5), suggesting that cobalt and iron particles did not undergo migration or aggregation during the process. It is evident that having a concentration of 10% and 20% borax caused a decrease in the intensity of the characteristic diffraction peaks associated with mAgnetite and fayalite phases, while also resulting in the appearance of a metallic iron phase (Figure 5). When the borax addition was increased to 30%, the diffraction peaks of fayalite disappeared, the peaks of mAgnetite were considerably reduced, and the peak of metallic iron became more pronounced, indicating a complete transformation of the silicate phase. For example, the peaks at 25.09°, 27.63°, 31.67°, 34.87°, 35.84°, and 65.96°, which correspond to Fe_2SiO_4,

gradually disappeared as the borax addition increased from 0 to 30%. The intensity of the peaks for mAgnetite at 29.71°, 35.55°, and 56.38° decreased significantly as the borax addition increased from 0 to 30% (Figure 5). This suggests that most of the fayalite phases were transformed into metallic phases, which is advantageous for the subsequent leaching process. According to Zhang et al. [6], the use of alkali disaggregation with CaO promotes the transformation of fayalite to mAgnetite, implying that the binding relationship between minerals and heavy metals in copper slag can be reduced from strong to weak. The primary factor responsible for the significant influence of $Na_2B_4O_7$ in this study was the sodium ions, which can infiltrate the crystal structure of Fe_2SiO_4 and lead to the formation of amorphous $Na_2O.SiO_2$. Hannon et al. [21] classified Na_2O as a network modifier and determined that SiO_2 consists of a fully interconnected network of SiO_4 tetrahedra, where pairs of tetrahedra are linked by the sharing of bridging oxygen (BO). The silicon atoms in the Fe_2SiO_4 structure act as network formers. When Na_2O is added to a silicate network, it causes the transformation of one bridging oxygen (BO) into two non-bridging oxygens (NBOs). The NBO plays a pivotal role in reducing the symmetry of Fe_2SiO_4 by incorporating alkali sodium ions into the amorphous silica network [22]. Thus, the utilisation of borax in the CCR process facilitates the conversion of fayalite into mAgnetite and metallic phases, thereby enhancing the extraction of critical metals.

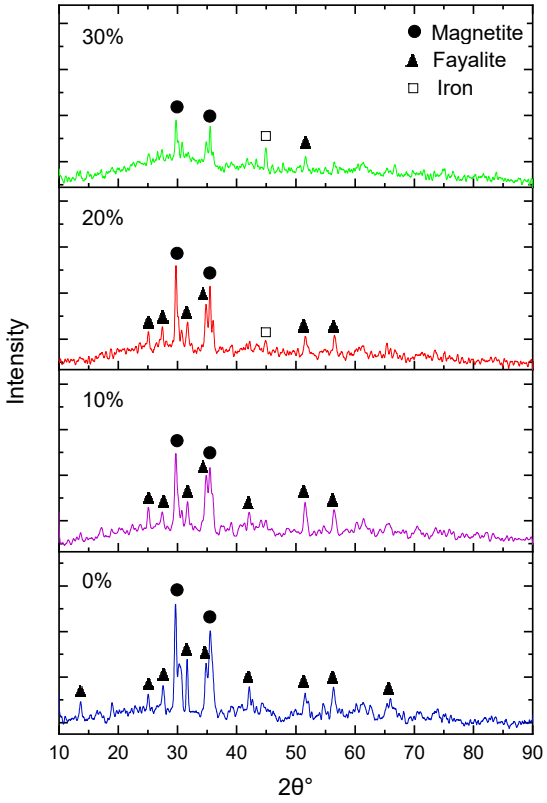

Figure 5. Effects of borax dosage on the reduction of the copper slag with 10% charcoal at 850 °C.

3.3.3. Effect of Reduction Temperature on Phase Transformation

To examine the phase transformation occurring during carbocatalytic reduction at various temperatures, the reduction temperature was set within the range 800 to 1000 °C. The other parameters, which included 10% charcoal, 20% borax, and 90 min reduction time, were kept constant. The XRD patterns of the products are depicted in Figure 6. At a reduction temperature of 800 °C, the conspicuous diffraction peaks of fayalite and mAgnetite exhibited a slight decrease following reduction (Figure 6). When the temperature was increased to 850 °C, 900 °C, and then to 950 °C, the diffraction peaks of fayalite and mAgnetite peaks became less pronounced, and the metallic iron phase became stronger. At a

temperature of 1000 °C, all fayalite and mAgnetite phases completely disappeared except for a minor mAgnetite phase peak at 29.83°, while the metallic iron phase became the predominant phase (Figure 6). The increase in the characteristic peak associated with metallic iron at an angle of 2θ = 44.93° indicated the occurrence of a redox reaction between Fe_2SiO_4 and $Na_2B_4O_7$. The results demonstrated that fayalite crystals underwent depolymerisation when the reduction temperature was increased. The rise in temperature intensified the reduction reaction between $Na_2B_4O_7$ and silicate compounds in the copper slag, resulting in the formation of polymeric sodium metasilicate anion and metallic phases. This is due to the fact that raising the temperature results in an increase in the equilibrium amount of metallic phases. Our previous study revealed that the formation of sodium metasilicate increased the equilibrium concentration of carbon monoxide (CO), facilitating a spontaneous reaction (Phiri et al., 2023). Partial pressure of CO increases above 800 °C and becomes the predominant phase in the reaction at elevated temperatures. The reason for this is that raising the reduction temperature enhances the potency of the Boudouard reaction ($C + CO_2 = 2CO$). Therefore, higher temperatures accelerate the transformation of fayalite, sulphides, and oxide phases into metallic phases. The diffraction peaks of sulphides and oxide minerals were not observed, which mAy imply that their quantities were insufficient for detection by XRD.

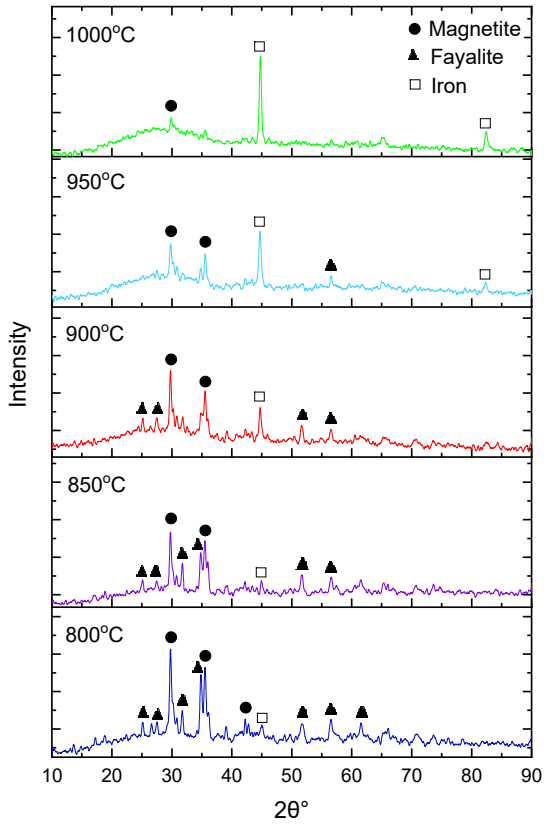

Figure 6. Effect of reduction temperature on the copper slag with 10% charcoal and 20% borax.

3.3.4. Comparison of Sulphuric Acid Leaching of the Feed Sample and Reduction Product

The feed sample with less than 75 µm particle size was first leached in 2 M H_2SO_4 for 90 min at room temperature (25 °C) with a liquid–solid ratio of 4 mL/g. The product after the carbocatalytic reduction process was also leached under the same optimum conditions. The results of the feed sample and the product after the carbocatalytic reduction process were then compared according to Figure 7.

Figure 7 depicts the metal extraction of a feed sample yielding 58.13% Cu, 32.58% Co, and 29.52% Fe. The low extractions of Co and Fe could be attributed to the fact that these metals are encapsulated in the silicate structure and cannot be dissolved in H_2SO_4

solution. Copper extraction was slightly higher because most of the copper in the copper smelting slag was found in the copper mAtte phase, which can be easily dissolved in H_2SO_4. Following the carbocatalytic reduction process, the extraction of Cu, Co, and Fe improved substantially, with mAximum efficiencies of 84.23% Cu, 87.13% Co, and 87.55% Fe. This suggests that the reduction process effectively disintegrated the fayalite structure, releasing Co and Fe metals that could then be leached in H_2SO_4. Thus, at optimum conditions, the carbocatalytic reduction process improved Cu, Co, and Fe extraction by 26%, 55%, and 58%, respectively. Our previous study (Phiri et al., 2023) provided a comprehensive analysis of the optimisation of charcoal addition, borax dosage, temperature, reduction, acid concentration, and leaching time.

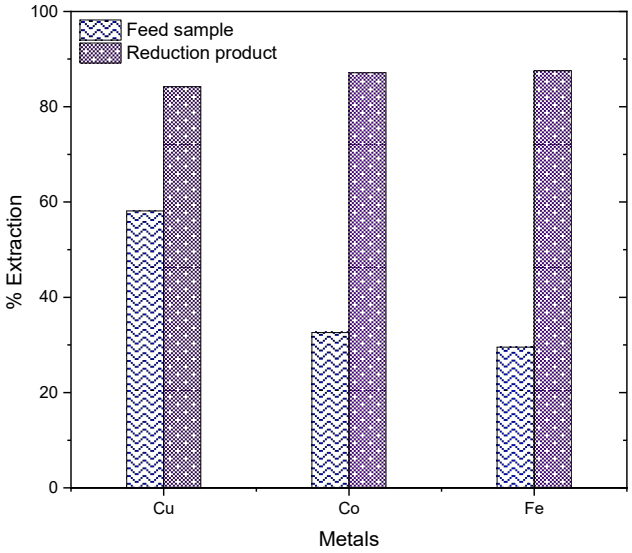

Figure 7. Comparison of metal extraction results of the feed sample and reduction product at optimum conditions (2 M H_2SO_4, 4 mL/g liquid to solid ratio, 90 min of leaching time at 25 °C).

3.3.5. Effect of Carbocatalytic Reduction on Metal Extraction by Leaching

Leaching experiments were conducted according to the procedure described in Section 2.3.2 to assess the efficacy of a carbocatalytic reduction (CCR) process of copper smelting slag for metal extraction. The leaching experiments were conducted on the product after carbocatalytic reduction (under optimal conditions of 10% charcoal dosage, 850 °C reduction temperature for 90 min) with variable borax dosage (0%, 10%, 20%, and 30%). The leaching conditions were 2 M H_2SO_4 with a liquid–solid ratio of 4 mL/g for 90 min at room temperature (25 °C). Figure 8 depicts the relationship between the efficiency of metal extraction and borax dosage.

Figure 8 shows that without borax addition, the total leaching efficiencies of Cu, Co, and Fe were 79.74%, 33.04%, and 28.35%, respectively. In comparison, at 10% borax addition, the corresponding total leaching efficiency for copper reached 86.99% Cu, while Co and Fe leaching efficiencies were significantly improved to 71.07% and 72.32%, respectively. The extraction of Co and Fe increased further as the borax dosage was increased to 30%, but the increase was insignificant, while copper extraction decreased. Although the borax mAy have little impact on copper reduction, as evidenced by a relatively high extraction without borax (0%) (Figure 8), increasing the borax to 30% mAy have provided a more reducing environment for copper metallisation, resulting in low extraction efficiency because copper metal cannot be leached in H_2SO_4. Thus, carbocatalytic reduction was most effective at disintegrating the fayalite structure containing cobalt and iron metals, resulting in the release of these metals, which were then leached in H_2SO_4. As a result, a 20% borax dosage was determined to be optimal, yielding mAximum efficiencies of 83.80% Cu, 84.75% Co, and 85.69% Fe.

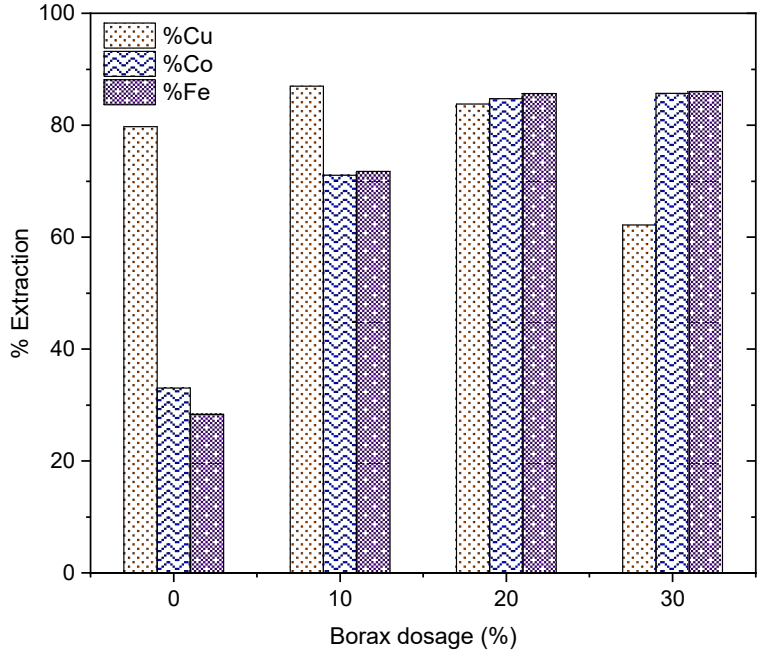

Figure 8. Effect of borax dosage on metal extraction using H_2SO_4 leaching (2 M H_2SO_4, 4 mL/g liquid to solid ratio, 90 min of leaching time at 25 °C).

Table 5 below presents the ICP-OES results for Cu, Co, and Fe in the leachate and leach residue on the carbocatalytic reduction product under optimum leaching conditions of 2 M H_2SO_4, 4 mL/g liquid to solid ratio, and 90 min of leaching time at 25 °C. The feed sample results have been included to demonstrate the mAss balance of the process.

Table 5. ICP-OES results of the feed, leachate, and the leach residue (wt.%).

Material Condition	Cu	Co	Fe
Feed	1.04	0.79	25.63
Leachate	0.87	0.67	21.96
Leach residue	0.17	0.12	3.67

4. Theoretical Basis for the Development of Carbocatalytic Reduction Technology for the Processing of Copper Slag

The critical determinant for carbocatalytic reduction (CCR) is the disintegration of the O-O bond in fayalite (Fe_2SiO_4) within the copper slag. Fayalite is an iron orthosilicate that has the crystal structure of olivine. The addition of charcoal (C) along with borax ($Na_2B_4O_7$) enhances the disintegration of Fe_2SiO_4 in the copper slag. The process of fayalite reduction by C entails the disaggregation of fayalite into silica and iron at the boundary between the silica-fayalite-iron phases. The hydrophobic nature of C allows for the direct interaction of silicate, which weakens the fayalite O–O bond. The presence of borax causes the O–O bond in fayalite to become even weaker by introducing a Na_2O modifier into a silicate network. The transformation of fayalite and cobalt silicate in the copper slag at low temperatures of 850 °C is illustrated according to Equations (1) and (2), respectively.

$$Fe_2SiO_4(s) + 2C(s) + Na_2B_4O_7(s) = Na_2O.SiO_2(s) + 2B_2O_3(s) + 2CO(g) + 2Fe(s), [\Delta G^\circ{}_{850\,^\circ C} = -37.224\ kj{\cdot}mol^{-1}] \quad (1)$$

$$Co_2SiO_4(s) + 2C(s) + Na_2B_4O_7(s) = Na_2O.SiO_2(s) + 2B_2O_3(s) + 2CO(g) + 2Co(s), [\Delta G^\circ{}_{850\,^\circ C} = -83.118\ kj{\cdot}mol^{-1}] \quad (2)$$

$$Co_2SiO_4(s) + 2CO(g) = 2Co(s) + SiO_2(s) + 2CO_2(g), [\Delta G^\circ{}_{850\,^\circ C} = -32.701\ kj{\cdot}mol^{-1}] \quad (3)$$

$$Fe_2SiO_4(s) + 2CO(g) = 2Fe(s) + SiO_2(s) + 2CO_2(g), [\Delta G^\circ{}_{850\,^\circ C} = +33.779\ kj{\cdot}mol^{-1}] \quad (4)$$

Thermochemical analysis indicates that fayalite reduction is thermochemically favourable as evidenced by a negative Gibbs free energy of reaction under ideal conditions ($\Delta G^{\circ}_{850\,^{\circ}C} = -37.224$ kj·mol^{-1}) (Equation (1)). Furthermore, the Gibbs free energy of Equation (2) exhibits a significantly negative value, indicating that the reduction of Co_2SiO_4 by charcoal in the presence of borax can occur spontaneously. In our previous study, we found that C dominates the reduction process at temperatures below 800 °C, whereas CO dominates the reduction reactions of fayalite at temperatures above 800 °C (Phiri et al., 2023). Equations (3) and (4) illustrate the reduction reactions of Co_2SiO_4 and Fe_2SiO_4 by CO, respectively. The Gibbs free energy of reaction implies that Equation (3) is thermochemically spontaneous at 850 °C, whereas Equation (4) is unfavourable at the same conditions.

Similarly, the direct reduction of mAgnetite to metallic iron using charcoal (C) is possible at the temperature of 850 °C according to Equation (5).

$$Fe_3O_4(s) + 4C(s) = 3Fe(s) + 4CO(g), [\Delta G^{\circ}_{850\,^{\circ}C} = -92.373\ \text{kj·mol}^{-1}] \quad (5)$$

While the copper sulphide reactions were exothermic at 850 °C, the chemical reactions with C were more favourable with $Na_2B_4O_7$ with $\Delta G^{\circ}_{850\,^{\circ}C} = +87.313$ kj·mol^{-1} (Equation (7)) than without $Na_2B_4O_7$ with $\Delta G^{\circ}_{850\,^{\circ}C} = +230.147$ kj·mol^{-1} (Equation (6)). This suggests that the presence of $Na_2B_4O_7$ and C could serve as a thermochemical driving factor.

$$Cu_2S(s) + C(s) = 2Cu(s) + CS(g), [\Delta G^{\circ}_{850\,^{\circ}C} = +230.147\ \text{kj·mol}^{-1}] \quad (6)$$

$$Cu_2S(s) + C(s) + Na_2B_4O_7(s) = Na_2S(s) + 2B_2O_3(s) + 2Cu(s) + CO(g), [\Delta G^{\circ}_{850\,^{\circ}C} = +87.313\ \text{kj·mol}^{-1}] \quad (7)$$

Our previous study described the thermochemical study of the direct reduction of mAgnetite and silicate compounds with charcoal in the presence of borax across a wider temperature range of 800–1000 °C [7]. Chemical reactions involving C were found to be more thermochemically spontaneous in the presence of $Na_2B_4O_7$ than in the absence of $Na_2B_4O_7$, implying that $Na_2B_4O_7$ is essential for the carbocatalytic reduction process. The addition of $Na_2B_4O_7$ to this reduction system significantly improves the thermochemical feasibility of carbocatalytic reduction of Fe_2SiO_4 and Co_2SiO_4. When $Na_2B_4O_7$ and C are added to copper slag, fayalite is completely transformed to sodium silicate and metallic iron (Equation (1)). Thermodynamic simulations using the HSC Chemistry 10 software [23] show that the CCR method allows for reduction reactions of fayalite and mAgnetite at substantially lower temperatures (850 °C) than conventional reduction processes. This could be due to the reaction products, sodium metasilicate ($Na_2O.SiO_2$) and boric oxide (B_2O_3), which have a low melting point and provide favourable reduction conditions for metal mAss transfer and aggregation. To further optimise this process, it is important to establish the mechanisms that facilitate the transformation of Fe_2SiO_4 and the formation of metallic phases during CCR. Figure 9 shows the mechanism of carbocatalytic reduction for processing the copper slag.

The CCR mechanism in Figure 9 has the potential to modulate the thermal degradation process and disintegrate the complex silicate-magnetite structure. The released valuable metals from smelting slag can then be extracted using hydrometallurgical techniques. When compared with high-temperature secondary processing of copper slag, this CCR process overcomes the inherent drawbacks of complex mineralogy and high-energy secondary processing without compromising efficacy.

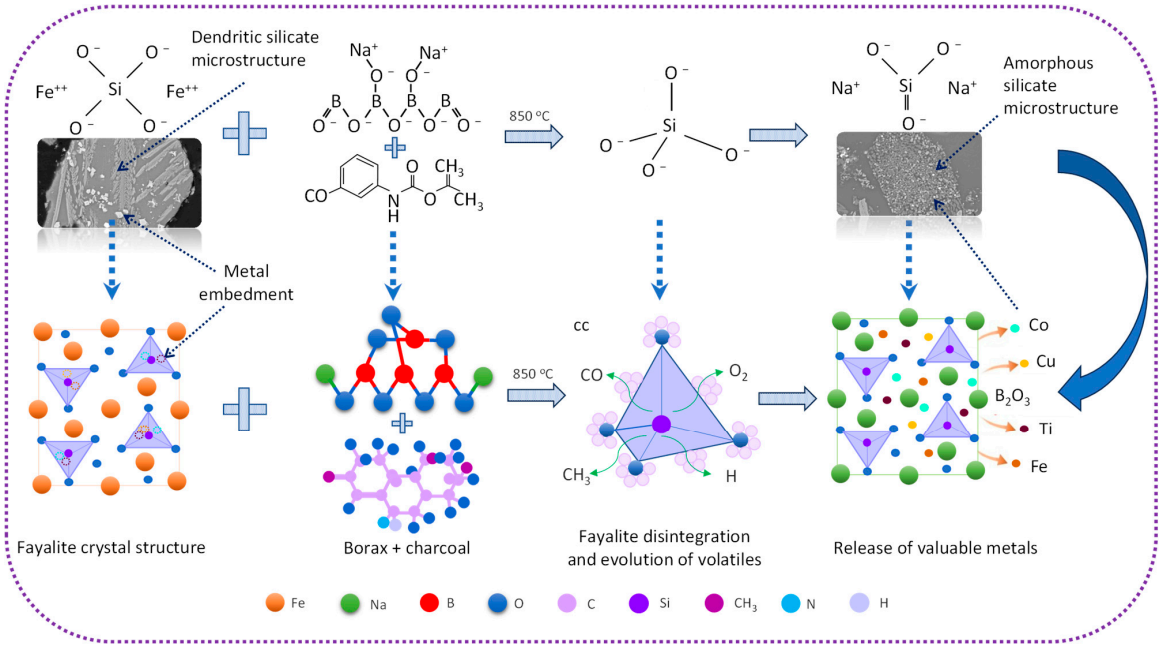

Figure 9. Mechanism and disintegration of fayalite by carbocatalytic reduction of the copper slag.

5. A Conceptual Flowsheet for Processing of Copper Smelting Slag

A conceptual flowsheet is proposed for processing copper smelting slag using a carbocatalytic reduction process, followed by hydrometallurgical extraction of Cu and Co and utilisation of the waste product. Figure 10 depicts the hypothetical flowsheet for the processing of copper smelting slag.

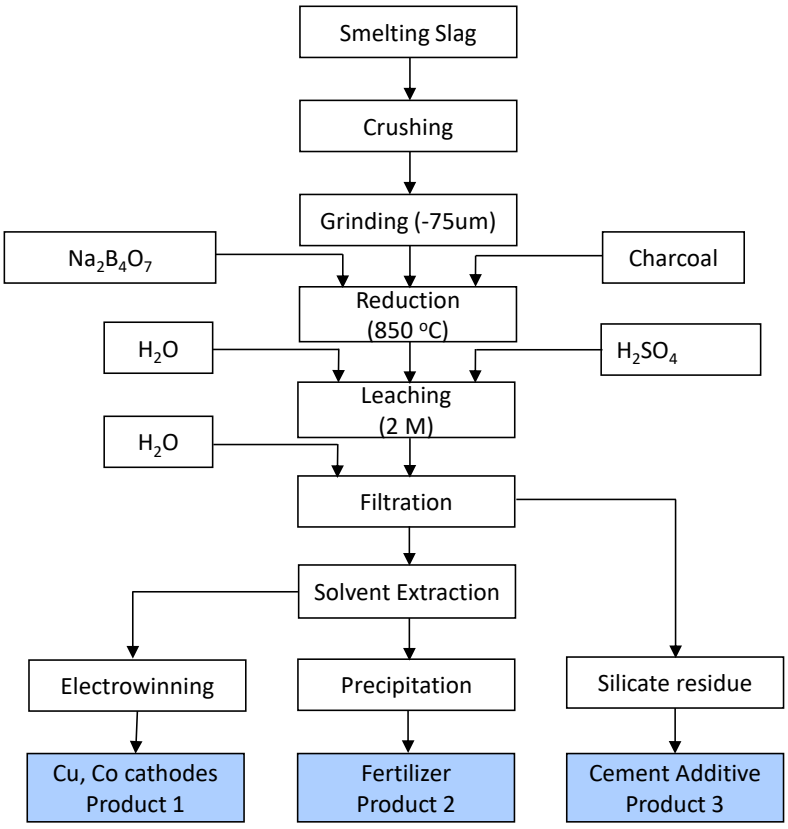

Figure 10. Conceptual flowsheet for carbocatalytic reduction and recovery of metals.

The conceptual flowsheet has been proposed based on the optimum conditions for the carbocatalytic reduction of copper slag and the leaching of the product using sulphuric acid. The smelting slag is first crushed, ground, and sieved to less than 75 μm. The milled slag is subsequently roasted at 850 °C using 10% charcoal and 20% borax. The product after the carbocatalytic reduction is then leached in 2 M H_2SO_4. After filtration, Cu, Co, and Fe can be extracted from the solution via the conversional solvent extraction technique. Copper and cobalt mAy be recovered using electrowinning to produce Cu and Co cathodes. Iron can be crystallised to produce iron sulphate, which is a valuable product. Then, other metals such as Al and Mg can be recovered through precipitation. The solid residue comprising silica and calcium can be separated by physical processes and utilised in construction as a cement additive. A comprehensive techno-economic analysis is required to assess the economic viability of the proposed flowsheet. To fully describe the mAss balance, further research into various metal recovery processes from solution is required.

6. Conclusions

In this study, the mineralogical characterisation of copper smelting slag and phase transformation after carbocatalytic reduction were investigated in order to develop an efficient metal extraction technique. The primary phases in the copper smelting slag were identified as silicate, mAgnetite, and copper using FESEM-EDS analysis. The silicate phase consisted of fayalite and kirschsteinite, while the copper phase was composed of copper mAtte and metallic copper. The FESEM-EDS results revealed that several metals, including Co, Cu, Fe, Si, Ca, Mg, Al, Ti, and K, were present in silicate and mAgnetite phases in significant concentrations. The Cu, Co, and Fe content distributions in the silicate phase were up to 5.08 wt.%, 1.44 wt.%, and 31.11 wt.%, respectively. The mAgnetite phase included up to 1.85 wt.% Co and 58.26 wt.% Fe. There was no copper detected in the mAgnetite phase. The copper mAtte had up to 73.52 wt.% Cu, 0.38 wt.% Co, and 11.01 wt.% Fe. The metallic copper phase was comprised of 89.62 wt.% Cu. The carbocatalytic reduction of copper slag has demonstrated efficacy in transforming the complex silicate-magnetite mAtrix into amorphous and metallic phases, mAking the extraction of metals easier. This is consistent with the XRD findings revealing that all fayalite and mAgnetite phases completely disappeared, while the metallic iron phase became the dominant phase. The addition of 20% borax to the reduction reactions allows for the disintegration of fayalite and mAgnetite at a significantly lower temperature of 850 °C than conventional reduction processes. Furthermore, the potential influence of carbocatalytic reduction on metal extraction in leaching experiments was investigated using 2 M H_2SO_4, resulting in mAximum extractions of 84.23% Cu, 87.13% Co, and 87.55% Fe. Thus, carbocatalytic reduction will contribute to the development of technology for extracting Cu and Co from copper smelting slag as well as reprocessing the accumulated slag waste for a more sustainable future.

Author Contributions: Conceptualization, T.C.P. and A.N.N.; Validation, P.S. and A.N.N.; Formal analysis, T.C.P.; Investigation, P.S. and A.N.N.; Resources, A.N.N.; Data curation, A.N.N.; Writing—original draft, T.C.P.; Writing—review and editing, A.N.N.; Supervision, P.S. and A.N.N.; Project administration, A.N.N.; Funding acquisition, A.N.N. All authors have read and agreed to the published version of the mAnuscript.

Funding: The Schlumberger Foundation Faculty for the Future Fellowship, and Murdoch University provided financial support for this research, which the authors gratefully acknowledge.

Data Availability Statement: The original contributions presented in the study are included in the article, further inquiries can be directed to the corresponding author.

Conflicts of Interest: The authors declare no conflict of interest.

References

1. Phiri, T.C.; Singh, P.; Nikoloski, A.N. The potential for copper slag waste as a resource for a circular economy: A review—Part I. *Miner. Eng.* **2022**, *180*, 107474. [CrossRef]
2. Piatak, N.M.; Parsons, M.B.; Seal, R.R. Characteristics and environmental aspects of slags: A review. *Appl. Geochem.* **2015**, *57*, 236–266. [CrossRef]
3. Phiri, T.C.; Singh, P.; Nikoloski, A.N. The potential for copper slag waste as a resource for a circular economy: A review—Part II. *Miner. Eng.* **2021**, *172*, 107151. [CrossRef]
4. Wang, D.W.; Zhao, Z.W.; Lin, Z.; Liang, Y.J.; Kang, L.; Peng, B. Interaction mechanism between arsenate and fayalite-type copper slag at high temperatures. Trans. *Nonferrous Met. Soc. China* **2022**, *32*, 709–720. [CrossRef]
5. Li, S.; Pan, J.; Zhu, D. A novel process to upgrade the copper slag by direct reduction-magnetic separation with the addition of Na_2CO_3 and CaO. *Powder Technol.* **2019**, *347*, 159–169. [CrossRef]
6. Zhang, S.; Zhu, N.; Shen, W.; Wei, X.; Li, F.; mA, W.; mAo, F.; Wu, P. Relationship between mineralogical phase and bound heavy metals in copper smelting slags. *Resour. Conserv. Recycl.* **2022**, *178*, 106098. [CrossRef]
7. Phiri, T.C.; Singh, P.; Yotamu, S.; Hara, Y.S.; Siame, J.; Nikoloski, A.N. Carbothermic Reduction of Copper Slag in the Presence of Borax. *Miner. Process. Extr. Metall. Rev.* **2023**, 1–12. [CrossRef]
8. Yamashita, T.; Hayes, P. Analysis of XPS spectra of Fe^{2+} and Fe^{3+} ions in oxide mAterials. *Appl. Surf. Sci.* **2008**, *254*, 2441–2449. [CrossRef]
9. Li, Y.; Perederity, L.; Papangelakis, V.G. Cleaning of waste smelter slag and recovery of valuable metals by presure oxidative leaching. *J. Hazard. mAter.* **2008**, *152*, 607–615. [CrossRef]
10. Zhang, H.; Hu, C.; Gao, W.; Lu, M. Recovery of Iron from Copper Slag Using Coal-Based Direct Reduction: Reduction Characteristics and Kinetics. *Minerals* **2020**, *10*, 973. [CrossRef]
11. Lan, C.; Zhang, S.; Liu, R.; Lyu, Q.; Yan, G.; Wang, B. Thermodynamic and kinetic behaviours of copper slag carbothermal reduction process. *Ironmak. Steelmak.* **2022**, *50*, 123–133. [CrossRef]
12. Guo, Y.; Zheng, F.; Jiang, T.; Chen, F.; Wang, S.; Qiu, G. Effects of Borax on the Reduction of Pre-oxidized Panzhihua Ilmenite. *JOM* **2017**, *70*, 2018.
13. Gorai, B.; Jana, R.K. Characteristics and utilisation of copper slag—A review. *Resour. Conserv. Recycl.* **2003**, *39*, 299–313. [CrossRef]
14. Vítková, M.; Ettler, V.; Johan, Z.; Kribek, B.; Sebek, O.; Mihaljevic, M. Primary and secondary phases in copper-cobalt smelting slags from the Copperbelt Province. *Zamb. Min. mAg.* **2010**, *74*, 581–600. [CrossRef]
15. Wu, L.; Wang, H.; Dong, K. Effect of Sulfur Content on Copper Recovery in the Reduction Smelting Process. *Metals* **2022**, *12*, 857. [CrossRef]
16. Mackwell, S.J. Oxidation Kinetics of Fayalite (Fe_2SiO_4). *Phys. Chem. Miner.* **1992**, *19*, 220–228. [CrossRef]
17. Đorđević, T.; Tasev, G.; Aicher, C.; Potysz, A.; Nagl, P.; Lengauer, C.L.; Pędziwiatr, A.; Serafimovski, T.; Boev, I.; Boev, B. Mineralogy and environmental stability of metallurgical slags from the Euronickel smelter, Vozarci, North Macedonia. *Appl. Geochem.* **2024**, *170*, 106068. [CrossRef]
18. Hu, J.H.; Wang, H.; Zhao, L.M.; Li, L.; Liu, H.L. Characterization of copper slag from impoverishment. *J. Saf. Environ.* **2011**, *11*, 90–93. [CrossRef]
19. Zhao, Z.; Wang, Z.; Peng, N.; Peng, B.; Liang, Y.; Qu, S.; Dong, Z.; Zeng, W. Copper behavior and fayalite microstructure changes influenced by Cu_2O dissolution. *JOM* **2019**, *71*, 2891–2898. [CrossRef]
20. Zhou, S.; Wei, Y.; Li, B.; Wang, H. Effect of Iron Phase Evolution on Copper Separation from Slag Via Coal-Based Reduction. *Metall. mAter. Trans. B* **2018**, *49*, 3086–3096. [CrossRef]
21. Hannon, A.C.; Vaishnav, S.; Alderman, O.L.G.; Bingham, P.A. The structure of sodium silicate glass from neutron diffraction and modeling of oxygen-oxygen correlations. *J. Am. Ceram. Soc.* **2021**, *104*, 6155–6171. [CrossRef]
22. Shi, G.; Liao, Y.; Su, B.; Zhang, Y.; Wang, W.; Xi, J. Kinetics of copper extraction from copper smelting slag by pressure oxidative leaching with sulfuric acid. *Sep. Purif. Technol.* **2020**, *241*, 116699. [CrossRef]
23. Kobylin, P.; Furta, L.; Vilaev, D. *HSC Chemistry 10; Equilibrium Module*; Metso Outotec: Espoo, Finland, 2021.